Properties of prompt-fission γ rays

I. Stetcu, P. Talou, T. Kawano, and M. Jandel

Phys. Rev. C **90**, 024617 — Published 26 August 2014

DOI: 10.1103/PhysRevC.90.024617

LA-UR-14-23128

Prompt fission γ-ray properties

I. Stetcu,[1] P. Talou,[1] T. Kawano,[1] and M. Jandel[2]

[1] *Theoretical Division, Los Alamos National Laboratory, Los Alamos, NM 87545, USA*
[2] *C-NR, Los Alamos National Laboratory, Los Alamos, NM 87545, USA*

In a Monte-Carlo Hauser-Feshbach statistical framework, we describe spectra, average multiplicities, average energy and multiplicity distributions of the prompt γ rays produced in the thermal neutron-induced fission of ^{235}U and ^{239}Pu, and the spontaneous fission of ^{252}Cf. Comparisons against recent experimental data show reasonable agreement in all cases investigated, after adjustment of the initial spin distribution in the fission fragments. In particular, when we include in the calculation the Doppler broadening we obtain a qualitatively good description of the measured low-energy spectra, where contributions from collective discrete transitions in specific fragments can be identified. At higher energies, both the calculated neutron and γ-ray spectra are softer than experimental data. The impact of selected model parameters on the prompt neutron and γ-ray spectra is analyzed. Finally, we present prompt γ spectrum and multiplicity distribution for the neutron-induced fission of ^{235}U for 5.5 MeV neutron incident energy, just below the threshold for second-chance fission.

PACS numbers: 25.85.Ec,24.75+i,24.10.Lx

I. INTRODUCTION

Properties of prompt fission neutrons and γ rays, emitted before the weak decays of the fission fragments toward stability, are important for both nuclear technologies and a better understanding of the fission process. Significant effort has been directed to the study of prompt fission neutron properties [1–5], in particular the average spectrum and multiplicity, but the properties of the prompt γ rays have been less studied. Hence, uncertainties on nuclear data needed for fast reactors are large, given that even in the well known thermal power reactors, the local γ heating can be under predicted by up to 30% [6]. The model used in this paper, based on a Monte-Carlo implementation [7, 8] of the statistical theory of Hauser and Feshbach [9], has a range of applicability well beyond thermal incident energies. However, in this paper, we study in detail the thermal-neutron induced fission of ^{235}U and ^{239}Pu, and the spontaneous fission of ^{252}Cf, where precise experimental data are available for comparison and benchmarking. We also present calculations for the neutron-induced fission of ^{235}U at 5.5 MeV incident energy, just below the second-chance fission threshold.

The excitation energy of the primary fission fragments is released mainly via neutron emission, followed by electromagnetic transitions to a more stable configuration, until a long-lived isomeric state or the ground state is reached. In principle, other particles or even clusters can be emitted, but they are highly suppressed due to Coulomb barrier. Both the neutrons and γ rays produced during the process, before any beta decays, carry information about the structure of the pre-neutron emission fragments. However, unlike the fission fragments, whose properties can be inferred only indirectly, the observables characterizing the prompt products can be directly measured, imposing stringent constraints on theoretical models that predict such observables.

In our approach, we consider each primary fission fragment as a compound nucleus, which de-excite via neutron and γ emissions. The path towards a long-lived state is followed in detail, using the Hauser-Feshbach equations to calculate the emission probabilities of neutrons and γ rays in competition, ensuring total energy conservation, while the spin and parity follow their respective conservation rules. The prompt neutrons carry most of the available excitation energy, but do not significantly modify the initial fragments' angular momenta. The spin is mostly removed by the γ emissions, dominated by statistical dipole transitions at higher energies and quadrupole transitions at low energies. The agreement with the measured prompt γ spectrum [10–16] is in general good, including a reasonable description of the features observed experimentally at low energies [10, 12–14], which are attributed to transitions between discrete levels of specific fragments. We also present in the current paper results for the multiplicity dependent spectrum and compare them against a parameterized model of the γ-ray emissions [15, 16]. Finally, in the regions where the agreement with experimental data is unsatisfactory, we investigate contributions from specific post-neutron emission fragments, in an attempt to diagnose the possible issues. Unfortunately, we cannot identify one single model parameter, or set of model parameters, that could improve our simulations' reliability.

The paper is organized as follows. In Sec. II we describe the Monte Carlo Hauser-Feshbach (MCHF) approach, discussing selected parameters and their expected influence on observables in Sec. III. In particular, we investigate the effect of the initial excitation energy sharing and spin distributions of the fission fragments, and energy cuts imposed by experimental constraints on prompt γ-ray average spectra and multiplicity. In Sec. IV we present in detail the results of our simulations which include average neutron and γ-ray multiplicity, average spectra, and average multiplicity and energy distri-

butions. We summarize and discuss future developments in Sec. V.

II. MODEL OVERVIEW

The Monte Carlo method used to simulate sequential emission of particles from excited fission fragments has been discussed in previous publications [1, 2, 4, 8, 17–19]. In our implementation, we make a couple of simplifying assumptions:

(i) particles are emitted only after the fission fragments have reached full acceleration;

(ii) no neutron is emitted during the nuclear system's evolution from saddle to scission, nor at the neck rupture;

The evidence for particle emission during the acceleration phase is not convincing, and recent work [20] has shown that the earlier interpretations of the observed neutron angular distributions are incorrect and should take into account the role of the moving fission fragments on the emission angles of the neutrons. It is highly probable that neutrons are emitted at scission, but with current information it is difficult to quantify their effect. Other observables, not discussed in this publication, could lead to a better understanding of this open question.

We further assume that the fully accelerated fission fragments can be treated as compound nuclei that can be modeled in a Hauser-Feshbach formalism. Thus, we bypass the complicated description of the scission process, and start the simulation by performing a Monte Carlo sampling of pre-neutron emission fission fragments from the yields as a function of mass (A), charge (Z), and total kinetic energy (TKE), denoted by $Y(A, Z, \mathrm{TKE})$. This process is non trivial given that no theoretical calculation of $Y(A, Z, \mathrm{TKE})$ exists and no experiment provides complete measurement of this quantity. While phenomenological models have been developed [21], in the current implementation we often combine experimental information from several sources. Thus, data on fission fragment yields and TKE distribution from different experiments is usually supplemented by systematics [22]. For details on how $Y(A, Z, \mathrm{TKE})$ is constructed, see, e.g., Refs. [4, 8]. On the theoretical front, some progress has been reported recently [23, 24], and in the future we should be able to use such models, if their associated uncertainties prove to be reasonably small.

Once $Y(A, Z, \mathrm{TKE})$ is determined, we use it to perform a Monte Carlo sampling of the primary fission fragments, obtaining a distribution of fragment pairs with fixed charges, masses and TKE. From the energy balance of the reaction, it is a simple exercise to determine the total excitation energy (TXE) available for particle emission in the two fragments. In the case of neutron-induced fission, TXE is given by

$$\begin{aligned} TXE = & M_n(A_l, Z_l) + M_n(A_h, Z_h) \\ & - M_n(A_c, Z_c) + E_{inc} + B_n(A_c, Z_c) - \mathrm{TKE}, \end{aligned} \quad (1)$$

where $M_n(A_l, Z_l)$ and $M_n(A_h, Z_h)$ are the nuclear masses of the light and heavy fragment respectively, $M_n(A_c, Z_c)$ is the mass of the compound fissioning nucleus, E_{inc} is the energy of the incident neutron, and $B_n(A_c, Z_c)$ is the binding energy of the neutron in the fissioning nucleus. For spontaneous fission, the energy associated with the incoming neutron in Eq. (1) is not present, so that TXE is simply obtained from

$$\begin{aligned} \mathrm{TXE} = & M_n(A_l, Z_l) + M_n(A_h, Z_h) \\ & - M_n(A_c, Z_c) - \mathrm{TKE}, \end{aligned} \quad (2)$$

and a similar equation determines TXE in the case of photofission, by adding the energy of the incoming photon to the energy balance. For both the spontaneous and γ-induced fission, the compound nucleus is the initial fissioning nucleus.

In order to start a Hauser-Feshbach simulation for each fragment, more information is required. This includes the initial excitation energy, initial spin and parity of each fragment. We simply assume that the parity distribution is equiprobable for positive and negative parities, but the problem of determining the partitioning of excitation energy sharing is more complicated and phenomenological models have been developed [4, 21, 25–27]. Similarly, for the initial spin distribution we use a simple model [28].

Because neutron emission is favored as long as the excitation energy is above the neutron separation energy, the available excitation energy in each fragment influences mostly the neutron observables. Hence, the average neutron multiplicity as a function of mass, for which some experimental data exist, can be used to constrain the theoretical models of energy sharing. In our approach, the energy sharing between the two fragments is parameterized by means of the ratio of the temperatures between light and heavy fragments, $R_T = T_l/T_h$. In the Los Alamos model [25], the initial assumption was that the two fragments are produced in thermal equilibrium, hence $R_T = 1$. Ohsawa and Shibata [29] obtained an improvement in the description of the prompt neutron spectrum by releasing the thermal equilibrium constraint and considering a mass-dependent ratio. In current calculations, R_T is also mass-dependent, and was fixed by fitting the ratio $\bar{\nu}_l/\bar{\nu}_h$ as a function of the fragment mass in a Weisskopf formalism [4].

The remaining unknown necessary to perform the Hauser-Feshbach simulations is the initial spin distribution of the fission fragments. While the spin cannot be directly measured experimentally, attempts to extract an average value have been done in the past from other fission observables like isomer production ratios [30, 31], γ-ray de-excitation feeding patterns of the ground-state bands [32] and angular anisotropy of prompt-fission γ

rays [33]. However, the extraction of the initial spin remains model dependent and often rely on simplified statistical models [34, 35], in which γ emission is modeled by means of counting and angular momentum algebra [34]. Moreover, our calculations have shown that in practice the large uncertainties in the experimental isomer production ratios, or the incomplete determination of the nuclear structure of the post-neutron emission fragments, which are predominantly far from stability, render very difficult the precise determination of the average angular momentum of the initial fragments [36]. Even in the simpler case of thermal neutron capture calculations are only in fair agreement with the experimental data [36].

In the absence of detailed information about the spin distribution, we assume that this is given by a Gaussian [28]

$$P(J) \propto (2J+1)\exp\left[-J(J+1)/2B^2(Z,A,T)\right], \quad (3)$$

where the spin cutoff parameter B is defined in terms of the fragment temperature T and the ground-state moment of inertia $\mathcal{I}_0(A,Z)$ of the fragment with mass A and atomic number Z

$$B^2(Z,A,T) = \alpha\frac{\mathcal{I}_0(A,Z)T}{\hbar^2}, \quad (4)$$

with α an adjustable parameter that we can fit to reproduce selected observables. Unlike in our previous publication [36], where we have attempted a determination of α from experimental information on isomer production ratios for selected isotopes, in this paper we consider α as a global parameter chosen to obtain the best description of the existing data on γ-ray spectra and multiplicity only. However, we have to point out that although α controls the angular momentum, which has little influence on the neutron emission, a weak dependence on the neutron average multiplicity ($\bar{\nu}$) still exists. This is due to the competition between neutron and γ emissions, which increases with increasing the angular momentum (see Fig. 4 in Ref. [8]). And because $\bar{\nu}$ is a very precisely measured quantity, a fine tuning of α is required for a good description of this quantity. In Sec. IV we will investigate the dependence on several γ-ray observables of the parameter α. For applications, we will recommend for each fissioning isotope the values that best describe measured quantities of interest, even if other observables might not be as well reproduced.

Once the initial conditions are fixed for each fragment, we use the Hauser-Feshbach statistical approach to model the de-excitation to a stable configuration. Thus, in the fragment's fixed system, the probability to emit a neutron of energy ε_n is given by

$$P_n(\varepsilon_n)d\varepsilon_n \propto T_n(\varepsilon_n)\rho(Z,A-1,E-\varepsilon_n-S_n)d\varepsilon_n, \quad (5)$$

while the probability to emit a photon with energy ε_γ by

$$P_\gamma(\varepsilon_\gamma)d\varepsilon_\gamma \propto T_\gamma(\varepsilon_\gamma)\rho(Z,A,E-\varepsilon_\gamma)d\varepsilon_\gamma. \quad (6)$$

Here E is the pre-neutron/γ emission excitation energy of the nucleus characterized by mass and atomic numbers A and Z respectively, S_n is the neutron separation energy. ρ stands for the density of states for the same nucleus (if a γ ray is emitted) or in the daughter nucleus (if a neutron is emitted), while $T_{n,\gamma}$ are the transmission coefficients for neutron/γ emission. In the case of neutrons, the transmission coefficients are determined from an optical potential model, and in this investigation we use the global optical potential of Koning and Delaroche [37]. For γ rays, the transmission coefficient is extracted from the γ-ray strength function $f_\gamma(\varepsilon_\gamma)$ assuming the Brink hypothesis [38] and using the Kopecky-Uhl formalism [39]

$$T_\gamma(\varepsilon_\gamma) = 2\pi\varepsilon_\gamma^{2L+1}f_\gamma(\varepsilon_\gamma), \quad (7)$$

where L is the multipolarity of the electromagnetic transition. We consider only $E1$, $M1$ and $E2$ transitions, employing the standard RIPL-3 parametrization [40] of the strength functions. For the transitions between the discrete levels, we use the experimental branching ratios available in the RIPL-3 compilation [40]. Finally, the nuclear density of states is constructed in the Gilbert-Cameron formalism [41].

For a given initial excitation energy, the total transition probability into all available states is normalized to one, and then, from the probability distribution, we sample the final state and implicitly the emitted particle. The particles are emitted sequentially until a stable configuration is reached, either in the form of the ground state, or a long-lived isomer.

As most quantum systems, the energy spectrum of each nucleus is in general composed of the discrete and continuum regions. We use the available experimental discrete levels, including the decay branching ratios, to model the discrete region. Above the last known discrete level we simulate the continuum using the level density formalism, matching the level densities to the discrete levels. The separation between the two zones highly depends on the level of experimental information. Because the fission fragments are created far from stability, the information is often restricted to just a handful of states, and frequently the spin or/and parity assignments are uncertain or completely missing. This can cause problems during simulation, because the spin is removed mainly by γ emission, as mentioned earlier. Thus, if we start with a high spin, as it seems to be required to obtain good agreement with $\bar{\nu}$ [8], one often reaches the discrete-continuum boundary in a state with large angular momentum, which would require a large electromagnetic multipolarity for a transition to a known discrete level. Because that would be unlikely, low-energy γ rays are emitted in the attempt to reduce the spin. This artificially increases the low-energy γ emissions, thus increasing the average multiplicity. Our solution is to bypass the low probability of high multipolarity electromagnetic decays and force the transition on the state with the closest spin available. This issue is amplified by the uncertainty in spin assign-

ment of the experimentally determined discrete states. Hence, including continuum-to-continuum or continuum-to-discrete γ rays with energies below about 100 keV reduces the reliability of our predictions. Motivated by this issue, and by the fact that experimentally it is difficult to measure γ rays below 100 keV, we exclude those from the analysis. However, we will show in the next section how our results for the average multiplicity in particular depend on the threshold. Thus, any meaningful comparison with experimental data has to take into account the energy interval in which the γ rays have been measured.

III. SENSITIVITY TO SELECT PARAMETERS

As discussed in the previous section, the MCHF description is phenomenological, relying on a large number of parameters. Some of them are "fixed" from systematics, like those describing the nuclear level densities, other can only indirectly be determined from their influence on fission observables. In this section, we investigate the sensitivity of selected observables to the choice of two important parameters that model the excitation energy sharing, R_T, and the initial angular momentum distribution, α. In addition, the influence of the low-energy cut, $E_{\rm cut}$, on the average γ-ray multiplicity is explored. For illustration we will show results only for ^{235}U$(n_{\rm th}, f)$, but the conclusions are general to all the reactions presented in the current investigation.

We start with the internal energy sharing, parameterized by the ratio between the light and heavy fragment temperatures, R_T. This parameter has little influence on global quantities, like the average total neutron multiplicity, or on γ observables, but it is essential in describing the mass dependence on the neutron observable. The excitation energy of each fragment is most efficiently released via neutron evaporation, until the excitation energy of the compound nuclei reaches the neutron separation energy. In that case, because the neutron emission becomes energetically impossible, the γ emission can proceed. The competition between neutrons and γ rays, which depends on the fragment's spin, sets the threshold for γ emission slightly above the neutron separation energy, but in general γ rays are seldom produced before neutrons. Hence, the total energy released via γ emission is about the same, no matter how the internal energy is shared, as long as the two fragments are excited above the separation energy. This heuristic argument is demonstrated in Fig. 1, where we present the average prompt γ multiplicity (a) and energy (b) as a function of the fission fragment mass number with two inputs for R_T: fixed $R_T = 1$ (thermal equilibrium between the fragments), and $R_T(A)$. For better illustrating the differences between the two calculations, we plot the ratio between their respective results. Since the ratio is close to one, with up to a 10% deviation, these observables are insensitive to the choice of R_T. This is in contrast with Fig. 2, where up to 40% deviation can be observed in the

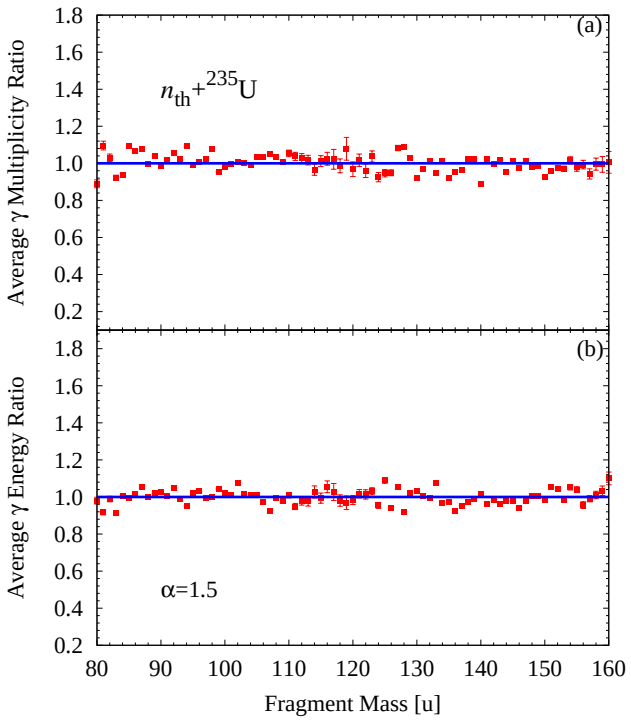

FIG. 1. (Color online) Prompt γ average multiplicity (a) and lab energy (b) as a function of the initial fragment. We present the ratio of the respective quantities for $R_T = 1$ to $R_T(A)$. In both calculations, the angular momentum distribution is set by $\alpha = 1.5$. A ratio of 1.0 would represent a perfect agreement between the two calculations.

average prompt-neutron multiplicity (a), for mass fragments 90–106 and 130–145 where the production yields are significantly larger than in the symmetric region. The parameter R_T controls the excitation energy sharing between the two fragments. While the excitation energy is strongly related to the multiplicity, the neutron energy depends on the temperature of the fragments, and, thus, shows a weaker dependence on R_T.

Another parameter that plays an important role in our simulations is α, which controls the initial angular momentum distributions of the primary fission fragments. In this case, for the same $R_T(A)$, calculations with different α show up to a 10% in the prompt neutron observables presented in Fig. 3. Moreover, the average neutron multiplicity varies slowly with α. The reason is that the neutron emission is only weakly influenced by the angular momentum, because it controls the competition between neutrons and γ rays [42]. To quantify the dependence, we have performed a quadratic fit, which gives $\bar{\nu}(\alpha) = 0.003\,\alpha^2 - 0.25\,\alpha + 2.83$ for ^{235}U$(n_{\rm th}, f)$. This α dependence, while weak, shows that a good description of $\bar{\nu}$ in this case is achieved for $\alpha \approx 2$. However, in order to better reproduce properties of the γ-ray spectra, especially the high-energy tail, we will choose smaller values for α, as argued in Sec. IV.

Increasing the initial angular momentum of the fission

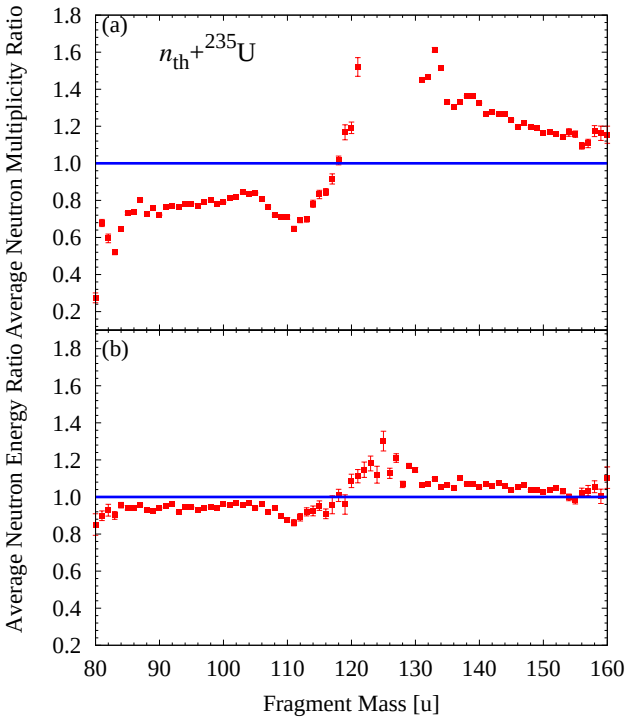

FIG. 2. (Color online) Same as in Fig. 1, but for prompt neutrons.

fragment will produces more γ rays along the path to a stable configuration. In Fig. 4 we show that increasing α, and, hence, the average initial angular momentum, increases the number of γ rays emitted by each fragment, by up to 40% for the initial fragments with significant yields. Hence, since the total available γ energy is the same we observe a decrease in the average γ-ray energy. Figure 5, representing the prompt γ multiplicity distribution, also illustrates an increase in the average prompt γ multiplicity caused by the larger initial average angular momentum. Thus, the average γ multiplicity increases from about 4.85 for $\alpha = 0.5$ to about 7.91 for $\alpha = 2$. We compare our results against the negative binomial model, which was proven to reproduce reasonably well the experimental data. In this model, the multiplicity probability distribution $P(N_\gamma)$ is given by [43]

$$P(N_\gamma) = \left(\begin{array}{c} \beta + N_\gamma - 1 \\ N_\gamma \end{array} \right) p^\beta (1-p)^{N_\gamma}, \qquad (8)$$

with β and p parameters determined from a fit to the experimental data. In this approach, β is related to the width of the distribution, while p is a function of β and the average multiplicity. It is difficult to obtain a good agreement with the negative binomial model if one uses the parameters of Valentine [43], as the multiplicity probability is very sensitive to the cutoff energy below which no γ rays are observed experimentally. Valentine relied on the available average γ multiplicity information at the time to extract his parameters, basing his fits on the data by Pleasonton [11], and Verbinski [12]. These data have a threshold of 90 keV and 140 keV, respectively, with comparable time-coincidence windows from the fission event of 5 ns and 10 ns respectively. In particular, Pleasonton data [11] is not compatible with the Peelle [10] and Oberstedt [14] measured multiplicities. As we will show below, the multiplicity, and, hence, the multiplicity distribution, are very sensitive to the threshold energy. We have also fitted the negative binomial model to our $\alpha = 1.7$ calculation, shown in Fig. 5 with a continuous line. In Table I we give the values of our parameters for the different reactions included in the paper. The multiplicity distribution obtained using the parameterized model of Jandel *et al.* [15, 16] requires a considerably smaller value of α, which would be incompatible with the successful description of other observables. However, the PM data follow more closely the Valentine evaluation.

TABLE I. Values for the β and p parameters resulting from a fit to our multiplicity distribution calculations performed with the optimal α parameters for each reaction, identified in Tables II and III

Reaction	β	p
^{235}U$(n_{\rm th}, f)$	10.91	0.59
^{239}Pu$(n_{\rm th}, f)$	13.17	0.64
^{252}Cf(sf)	15.39	0.65

The effect of α on the prompt γ energy spectrum is shown in Fig. 6 where we plot the ratio of the spectra for $\alpha = 0.5, 1.0, 1.5, 2.0$ to the spectrum obtained with $\alpha = 1.7$. It is difficult to quantify exactly what produces fewer γ rays at low energies for $\alpha = 0.5$ compared with $\alpha = 1.7$, as the results are depend on the level densities, strength functions and initial angular momentum in a large number of nuclei. While we do expect more γ rays with increasing the initial angular momentum, we cannot predict how those are distributed. The only artifact of our calculation was discussed in the previous section, and it regards the emission of low-energy γ rays at the threshold between the continuum and the discrete spectra. To eliminate those, we impose a cutoff energy $E_{\rm cut}$. Unless otherwise noted, we will present results for $E_{\rm cut} = 100$ keV.

The threshold is also motivated by the experimental resolution of different detectors, intrinsic to the experimental measurements. In Tables II and III, we present the results for two integral quantities, the average total γ multiplicity per fission and the average γ-ray energy, as a function of the threshold energy $E_{\rm th}$. We also present experimental results obtained with the same energy threshold of the detectors. In the case of DANCE, we do not present the experimental data, but rather the results of the parameterized model (PM) that was shown to reproduce the experimental data very well [15, 16]. Such a model was constructed to reproduce the total γ-ray energy spectra, and cannot be expected to reproduce

TABLE II. Average γ-ray multiplicity $\langle M_\gamma \rangle$ as a function of the low-energy threshold and spin parameter α, in the thermal neutron-induced fission of ^{235}U and ^{239}Pu, and the spontaneous fission of ^{252}Cf. We also show data from various experiments and the multiplicity in the parameterized model (PM).

$E_{\rm ct}$ [MeV]	α					PM	Exp.
	0.5	1.0	1.5	1.7	2.0		
^{235}U$(n_{\rm th}, f)$							
0.1	4.85	6.04	7.04	7.41	7.91	6.23	8.19±0.11 [14]
							6.51 ± 0.31 [11] [a]
0.14	4.62	5.73	6.65	6.99	7.46	6.18	7.45 ± 0.32 [10]
							6.69 ± 0.30 [12]
							7.78 [b]
0.3	3.94	4.76	5.43	5.68	6.02	5.68	6.11[b]
1.0	1.93	2.10	2.24	2.29	2.35	2.34	2.33 [b]
2.0	0.69	0.67	0.66	0.66	0.66	0.67	0.69 [b]
^{239}Pu$(n_{\rm th}, f)$							
0.1	5.57	6.95	7.48	7.87	8.39	7.08	7.38 [c]
0.14	5.25	6.52	7.05	7.39	7.88	7.01	7.23 ± 0.30 [12]
0.3	4.40	5.34	5.72	6.38	6.33	6.44	5.95[c]
1.0	2.15	2.36	2.39	2.56	2.51	2.79	2.17 [c]
2.0	0.76	0.75	0.74	0.74	0.74	1.06	0.72 [c]
^{252}Cf(sf)							
0.1	5.52	6.74	8.04	8.15	8.68	8.02	8.30 ± 0.08 [13]
0.14	5.23	6.34	7.51	7.64	8.12	7.89	7.8 ± 0.3 [12]
							8.01 [d]
0.3	4.23	5.02	5.86	5.95	6.29	6.83	6.45 [d]
1.0	1.99	2.14	2.31	2.33	2.40	2.22	1.90 [d]
2.0	0.73	0.73	0.74	0.74	0.74	0.77	0.67 [d]

[a] The threshold energy for this measurement is 90 keV.
[b] Calculated from the data by Oberstedt *et al.* [14] by integrating the spectrum measured with the $LaBr_3$ detector over the appropriate energy range.
[c] Calculated from the ENDF/B-VII.0 evaluation by integrating the spectrum. Note that the ENDF evaluation is based on the data by Verbinski *et al.* [12].
[d] Calculated from the data by Billnert *et al.* [13] by integrating the spectrum measured with the $LaBr_3$ detector over the appropriate energy range.

the detailed fluctuations observed below 1.5 MeV in experiments [12–14] and in our calculations of the γ-ray energy spectra. Nevertheless, PM provides a reasonable estimate of the average spectra and we will use it for comparison. This is especially useful in the case of exclusive energy spectra for distinct multiplicities, which can be produced in our simulation and have not been measured in any other experiments. Hence, it can provide a useful test of our model, even though the average multiplicities are systematically underestimated, while the average γ-ray energies are overestimated with respect to the latest measurements in the case of ^{235}U [14] and ^{252}Cf [13] respectively.

For the ^{235}U$(n_{\rm th}, f)$ reaction, we plot in Fig. 7 the average γ multiplicity and energy as a function of the threshold energy. This shows a strong average γ-ray multiplicity dependence on the threshold energy. In particular at low energies we find a large spread not only for our calculations with different initial average angular momentum, but also for the experimental data. Given the inconsistencies between the experiments, we cannot chose a α value based on the average γ-ray multiplicity alone. Thus, because higher α values produce softer γ-ray spectra, we have chosen $\alpha = 1.7$ as a compromise value, even though $\alpha = 2$ gives an average γ-ray multiplicity closer to the Oberstedt measurement. The same value is used for ^{252}Cf(sf), while for ^{239}Pu$(n_{\rm th}, f)$ we employ $\alpha = 1.5$. However, it should be noted that $\bar{\nu}$ requires about 30% higher values of α in all cases in order to achieve good agreement with the experiment and consistent with higher γ multiplicity.

Finally, another parameter to which both the theoretical simulations and experimental measurements are sensitive is the time coincidence window from the fission event when the γ rays are observed. We have obtained up to a 8% variation when the time window is changed from a few nanoseconds to a few seconds. This dependence is due to the finite halflife of certain states. Throughout

TABLE III. Same as in Table II, but for the average prompt-γ energy (in MeV).

$E_{\rm th}$ [MeV]	α					PM	Exp.
	0.5	1.0	1.5	1.7	2.0		
^{235}U$(n_{\rm th}, f)$							
0.1	1.06	0.95	0.88	0.87	0.85	1.03	0.85±0.02 [14]
							0.99 ± 0.09 [11] [a]
0.14	1.06	0.99	0.93	0.91	0.89	1.04	0.97 ± 0.05 [12]
							0.96 ± 0.05 [10]
							0.88 [b]
0.3	1.26	1.15	1.09	1.07	1.05	1.11	1.06 [b]
1.0	1.94	1.86	1.81	1.80	1.78	1.80	1.84 [b]
2.0	2.90	2.84	2.81	2.80	2.79	2.89	2.92 [b]
^{239}Pu$(n_{\rm th}, f)$							
0.1	1.07	0.96	0.89	0.88	0.85	1.14	0.91 [c]
0.14	1.11	1.00	0.94	0.92	0.90	1.15	0.94 ± 0.04 [12]
0.3	1.28	1.17	1.11	1.09	1.07	1.24	1.08 [c]
1.0	1.97	1.89	1.85	1.83	1.82	2.04	1.93 [c]
2.0	2.94	2.89	2.86	2.86	2.85	3.12	3.04 [c]
^{252}Cf(sf)							
0.1	0.99	0.90	0.84	0.84	0.82	0.90	0.80 ± 0.01 [13]
0.14	1.04	0.95	0.89	0.88	0.87	0.91	0.88 ± 0.04 [12]
							0.82[d]
0.3	1.23	1.14	1.08	1.07	1.06	1.02	0.96 [d]
1.0	1.97	1.91	1.86	1.86	1.85	1.90	1.91 [d]
2.0	2.92	2.88	2.87	2.86	2.86	2.90	2.83 [d]

[a] The threshold energy for this measurement is 90 keV.
[b] Calculated from the data by Oberstedt *et al.* [14] as the first moment of the spectrum measured with the $LaBr_3$ detector.
[c] Calculated from the ENDF/B-VII.0 evaluation as the first moment of the spectrum.
[d] Calculated from the data by Billnert *et al.* [13] as the first moment of the spectrum measured with the $LaBr_3$ detector.

the paper, we use 6 ns time windows, as this is what the latest measurements by Oberstedt and Billnert report. The other experimental data considered were measured for similar time windows, with the exception of data by Peelle et. al, for which 69 ns were reported [10].

IV. RESULTS AND DISCUSSION

In this section, we present results for ^{235}U(n, f), ^{239}Pu$(n_{\rm th}, f)$ and ^{252}Cf (sf). In the case of ^{235}U, we also show selected prompt γ observables for neutron-induced fission with the incident energy of 5.5 MeV.

A. Neutron-induced fission of ^{235}U

For the thermal neutron-induced fission of ^{235}U, we used the experimental information obtained with the double-sided Frisch-grid ionization chamber for $Y(A, \mathrm{TKE})$ [44], complemented by the Wahl systematics for the charge distribution [22]. The global parameter α has been chosen to be 1.7, as argued in the previous section.

In Fig. 8, we present a comparison of the calculated spectrum for ^{235}U$(n_{\rm th}, f)$ against experimental data and the ENDF B-VII.1 evaluation, which is based on the Verbinski data [12]. In order to make a meaningful comparison, we have scaled all the curves so that in the interval 0.3 – 5 MeV, they all have the same normalization. The low-energy part of the spectrum shows a remarkable agreement with the data by Verbinski [12] and Oberstedt [14], dominated by structures arising from transitions between discrete states. This is illustrated in Fig. 9, where we decompose the theoretical spectrum in contributions from continuum-to-continuum, continuum-to-discrete and discrete-to-discrete transitions. We obtain, however, a small shift toward lower energies for several of the peaks present in the experimental spectrum. The shift is systematic and appears for the other reactions investigated here. Hence, it is unlikely to be explained by small uncertainties in the discrete transitions taken from the RIPL3 database [40]. Further investigations are needed to find the source of the discrepancy.

We observe a reasonable agreement of the calculated spectrum with the experimental data up to 4.5 – 5 MeV.

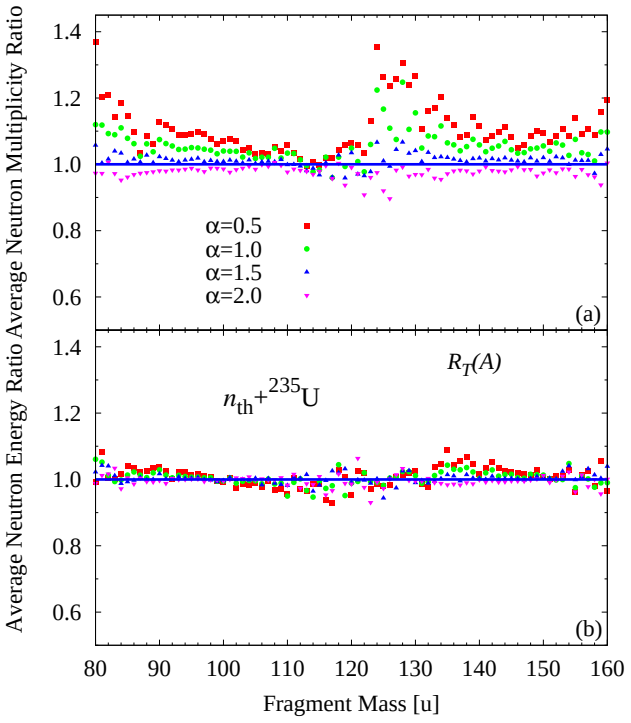

FIG. 3. (Color online) The prompt neutron average multiplicity (a) and energy (b) as a function of the initial fragment mass, for five values of the α parameter. As in Fig. 1, we plot the ratio of the results for $\alpha = 0.5, 1.0, 1.5, 2.0$ to the ones for $\alpha = 1.7$. In all calculations, the same $R_T(A)$ was used.

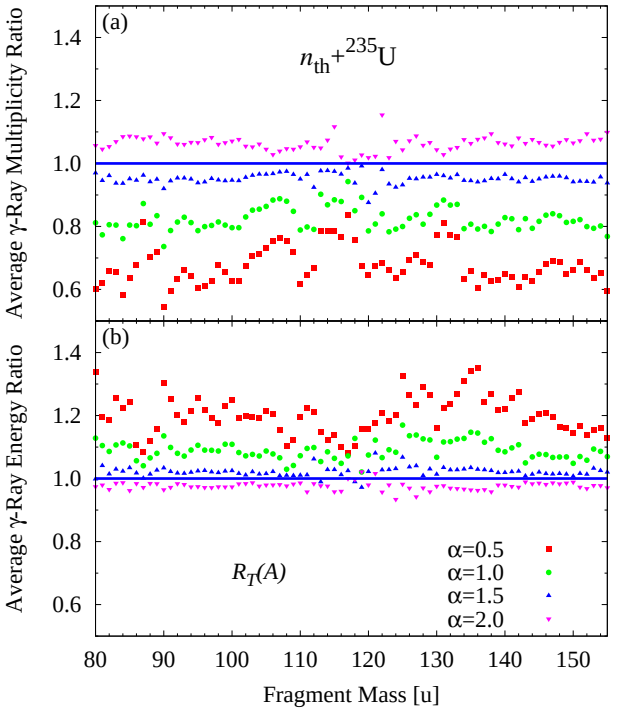

FIG. 4. (Color online) Same as in Fig. 3, but for prompt γ rays.

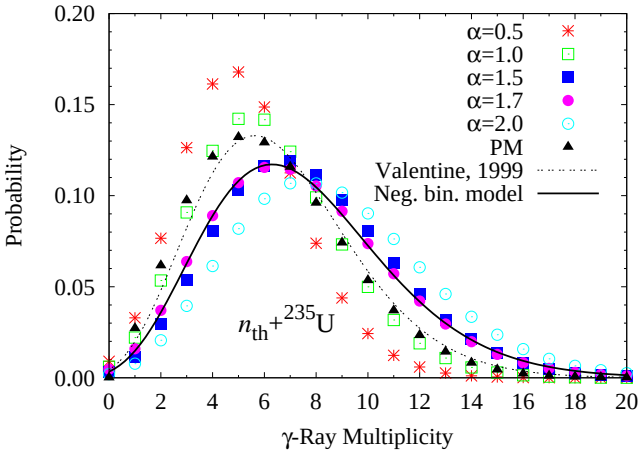

FIG. 5. (Color online) The prompt γ multiplicity distribution in MCHF for five values of the α parameter compared against the parameterized model (PM), the Valentine model [43], and the negative binomial model with the parameters fitted to our $\alpha = 1.7$ calculation.

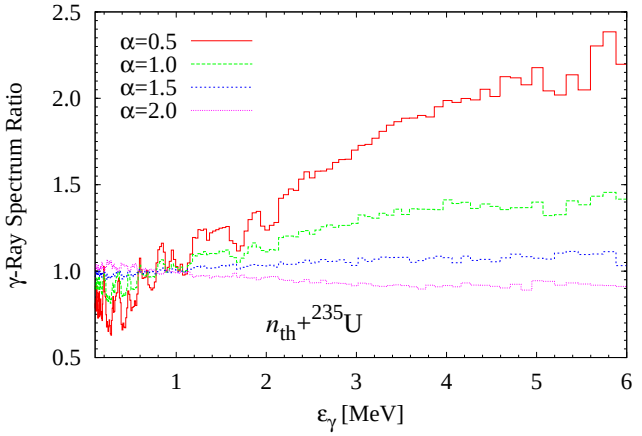

FIG. 6. (Color online) The prompt γ-ray energy spectrum calculated with MCHF, plotted as a ratio of the spectrum obtained with $\alpha = 0.5, 1.0, 1.5, 2.0$ to the result of $\alpha = 1.7$.

At higher energies, we obtain a spectrum that becomes softer than the experiment. Within the current implementation, using a smaller α hardens the spectrum, but other observables, like the average γ multiplicity or average γ energy presented in Tables II and III respectively, are poorly described. Our calculations are in agreement with the parameterized model at high energies, which is remarkable, given the fact that the model was developed for the total energy spectrum.

In Fig. 10, we present the average multiplicity (upper panel) and average individual γ-ray energy (lower panel) as a function of the fission fragment mass. We obtain the saw-tooth behavior and other features of the average multiplicity observed experimentaly. Thus, around fragment mass 85 we reproduce a drop in the average multiplicity that seems to be present in both the Pleasonton [11] and

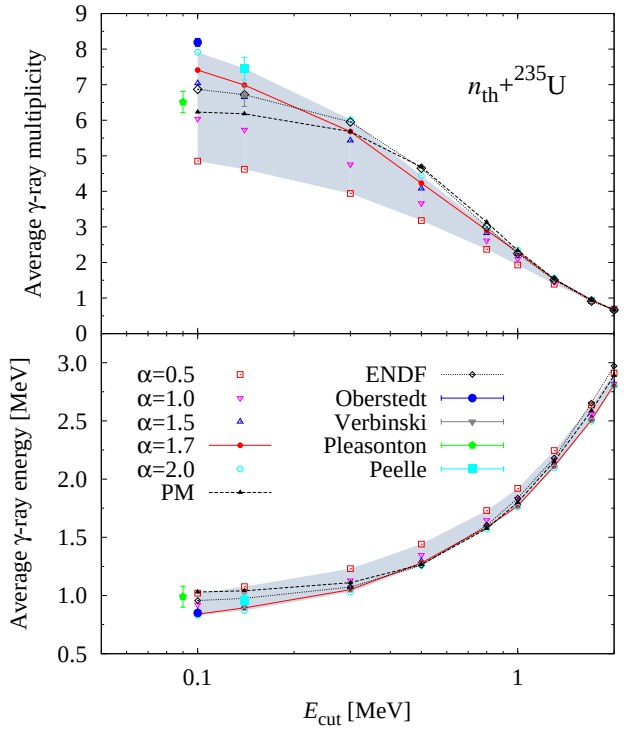

FIG. 7. (Color online) Dependence on average γ-ray multiplicity (upper panel) and average γ-ray energy of the threshold energy $E_{\rm cut}$ used in the calculation. The ENDF data was obtained by integrating the evaluated spectrum combined with the evaluated multiplicity. The filled area shows the spread in our calculations for different α parameters.

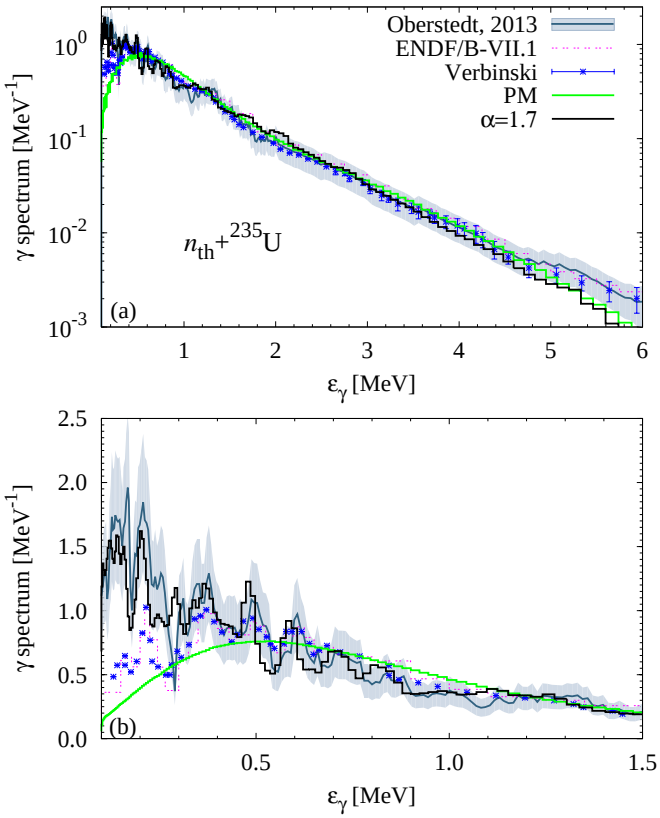

FIG. 8. (Color online) The prompt γ spectrum for $^{235}U(n_{\rm th}, f)$ (upper panel). Our calculation with $\alpha = 1.7$ is compared against the experimental spectra obtained by Verbinski [12] and Oberstedt [14], as well as against the parameterized model of Jandel et al. [16]. In the lower panel we present, in linear scale, the low-energy part of the spectrum, where discrete transitions play a major role.

Albinsson [45] data sets. Reasonable agreement of the Albinsson data can be also observed in the 130-140 mass region, as well as an apparent flattening of the multiplicity in the 140-155 mass region. In our previous publication [8], we have obtained an almost flat dependence of the multiplicity as a function of mass. The main difference is that in the present work we took into account the available lifetimes of all the states involved in the decay path, as compared to the observation time window, eliminating the transitions that are not likely to occur due to the time constraints. A reasonable description of the average individual γ-ray energy as a function of mass is shown in the lower panel of Fig. 10, where we reproduce well the peak around mass 130. This feature is a consequence of the decreased density of states around shell closure, which in turn increases the γ energy.

Exclusive prompt γ energy spectra for multiplicities 2, 4,... 20, are presented in Fig. 11, where we compare again our calculation against the results of the parameterized model. We obtain good agreement between all our simulations with different α parameters and the parameterized model for all multiplicities (including those not shown in Fig. 11). Thus, the agreement shown in this figure does not play a major role in the choice of α.

At the incident neutron energy of 5.5 MeV, we obtain results that are very similar to the case of thermal neu-

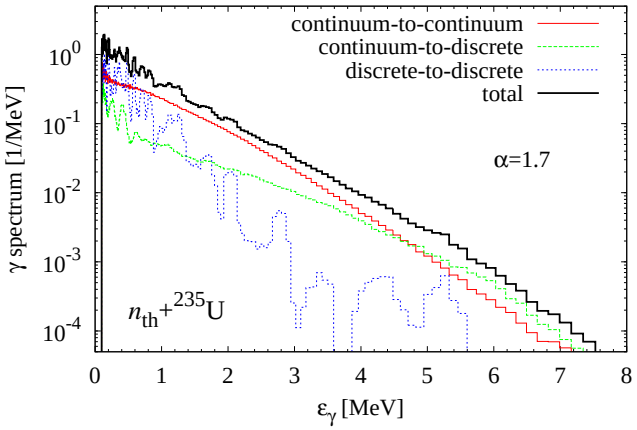

FIG. 9. (Color online) The prompt γ-ray energy spectrum decomposed into contributions from the continuum-to-continuum, continuum-to-discrete, and discrete-to-discrete transitions.

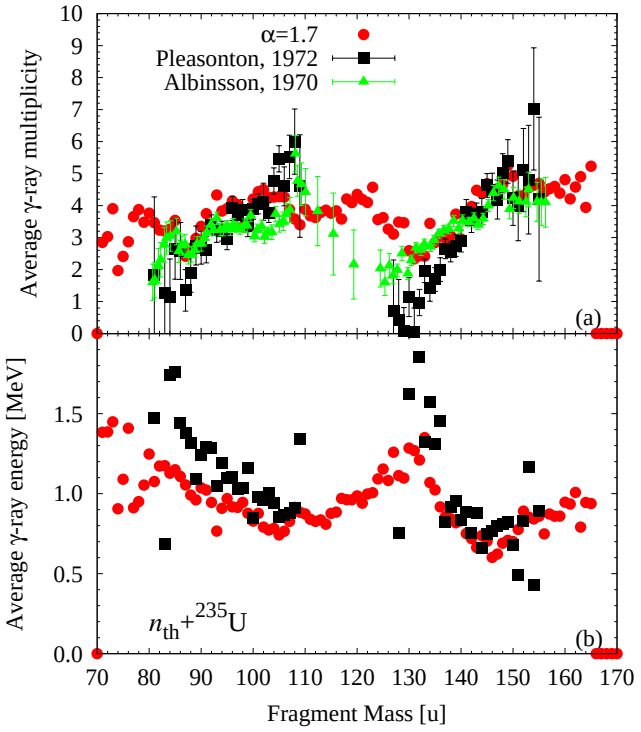

FIG. 10. (Color online) The average γ-ray multiplicity (a) and average γ-gamma energy (b) as a function of mass for ^{235}U$(n_{\rm th}, f)$.

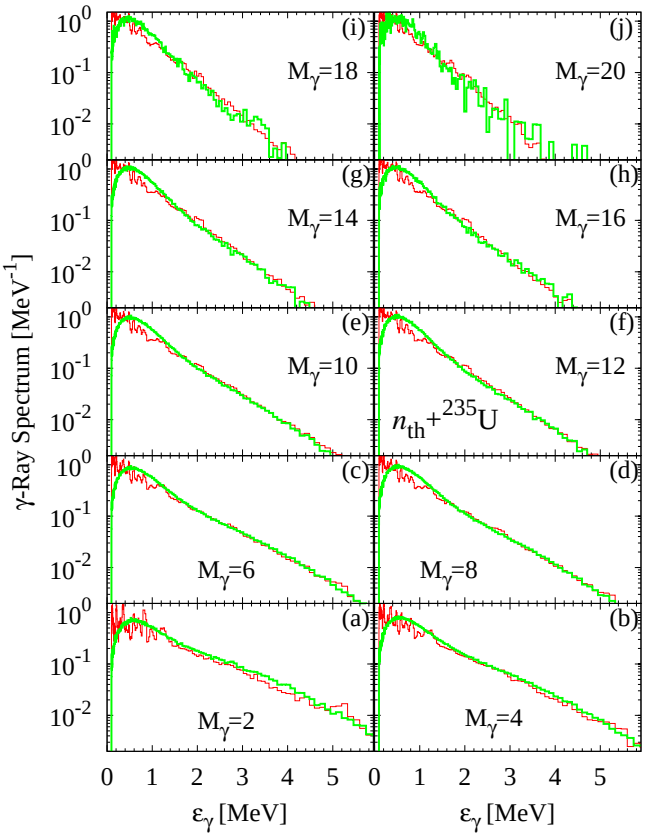

FIG. 11. (Color online) The prompt γ spectrum in the thermal neutron-induced fission of ^{235}U, for multiplicities 2, 4, 6,...20. We compare our results for $\alpha = 1.7$ against the parameterized model.

tron. In this case, we have used the pre-neutron emission yields provided by Hambsch et al. [46]. In Fig. 12 we show prompt γ spectra for both the thermal and 5.5 MeV incident neutron energies. The two spectra are very similar up to 4 MeV, while at higher energies the 5.5 MeV neutron spectrum is slightly harder than the thermal one. The multiplicity probability distribution for 5.5 MeV incident neutron energy for different values of α is shown in Fig. 13, where the results are similar to the ones presented in Fig. 5. In addition, the average γ-ray multiplicities shown in the legend are very similar to the values presented in Table II, for $E_{\rm cut} = 100$ keV.

Because the prompt neutrons are emitted before γ rays, we do expect that below the second-chance fission threshold the prompt γ observables will not present a strong dependence upon the incident energy. Most of the differences can come from the dependence on the incident energy of the pre-neutron emission yields and, possibly, from the initial angular momentum dependence on the incident energy. We incorporate, to some extent, an energy dependence in the initial spin distribution by assuming the temperature dependence of the spin cutoff parameter in Eq. (4). But because we have no information regarding α, we have taken the same value of 1.7 as in the case of the ^{235}U$(n_{\rm th}, f)$ reaction.

B. Neutron-induced fission of ^{239}Pu

If in the case of the ^{235}U$(n_{\rm th}, f)$ reaction we have directly used experimental data to determine the yields, for ^{239}Pu$(n_{\rm th}, f)$ the yields were reconstructed using partial data of mass-dependent yields and the mass-dependent average kinetic energy and its standard deviation [4]. As for ^{235}U, the Z-dependence is taken from the Wahl systematics [22].

Our results for the γ-ray energy spectrum and multiplicity probability distribution are shown in Figs. 14 and 15, respectively. In this case, conform to Tables II and III, we have chosen $\alpha = 1.5$, because it provides better agreement with the experimental data for the average multiplicity and photon energy of Verbinski *et al.* [12]. In addition, because in general a larger α parameter translates into a softer spectrum, and our calculations tend to be too soft at higher energies, we favor in this case a smaller value of α than for the ^{235}U$(n_{\rm th}, f)$ reaction.

The agreement we obtain with available data is reasonable for the energy spectrum, as it can be inferred from Fig. 14. As before, the spectrum becomes softer than the ENDF/B-VII.1 evaluation, although it remains closer to

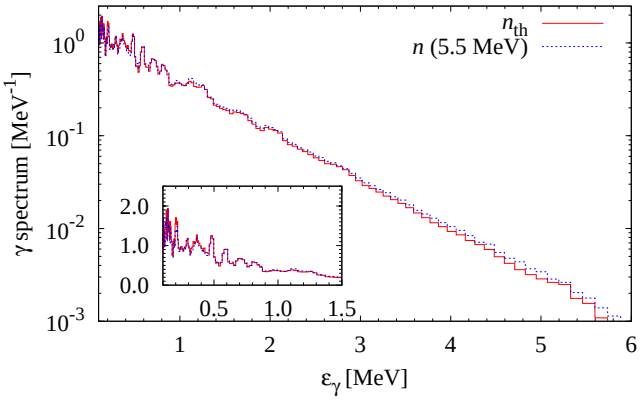

FIG. 12. (Color online) Comparison between the prompt γ spectra for the induced fission of ^{235}U by thermal neutrons (continuous line) and by neutrons with 5.5 MeV incident energy.

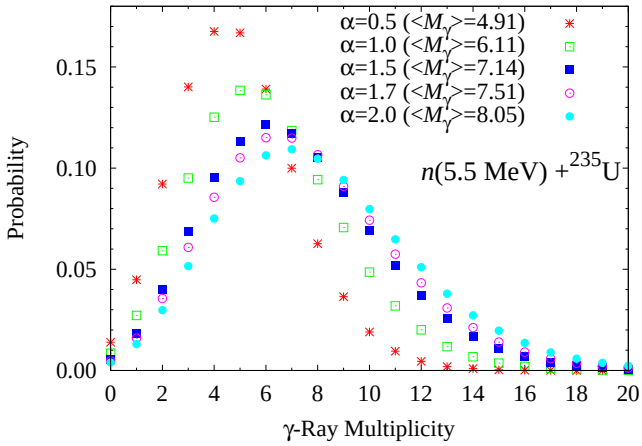

FIG. 13. (Color online) Comparison between the prompt γ multiplicity distribution for the induced fission of ^{235}U by thermal neutrons (continuous line) and by neutrons with 5.5 MeV incident energy.

the parameterized model simulation. For the multiplicity probability distribution shown in Fig. 15, we find, as in the ^{235}U$(n_{\rm th}, f)$ case, that the Valentine model agrees better with the Ullmann measurement [15] than with our calculation.

C. Spontaneous fission of ^{252}Cf

The same Monte-Carlo Hauser Feshbach formalism can be applied to describe properties of prompt neutrons and γ rays produced in the spontaneous fission of ^{252}Cf. In this case, we have employed the fission yields measured using the double-sided Frisch-grid ionization chamber [44, 46]. As for the previous reactions, we have used the Wahl systematics for the charge distribution [22]. The input parameter that controls the angular momentum has been chosen to be $\alpha = 1.7$, as for the ^{235}U$(n_{\rm th}, f)$

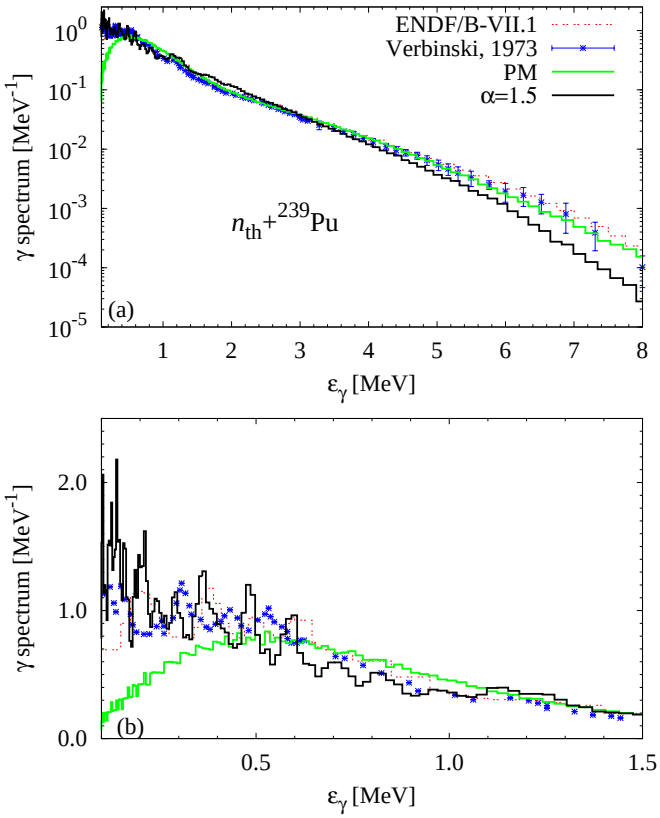

FIG. 14. (Color online) The prompt γ spectrum for $^{239}Pu(n_{\rm th}, f)$. Our calculation with $\alpha = 1.5$ is compared with the experimental spectrum measured by Verbinski *et al.* [12], as well as with the parameterized model of Jandel et al. [15]. In the lower panel, we present, in linear scale, the low-energy part of the spectrum, where discrete transitions can be identified as in Fig. 8.

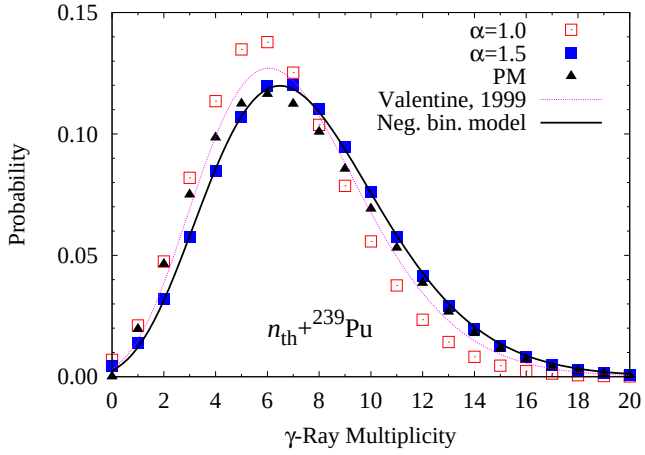

FIG. 15. (Color online) The prompt γ multiplicity distribution in MCHF for $\alpha = 1.5$ compared with the parameterized model (PM), Valentine model [43], and the negative binomial model with the parameters fitted to our optimal calculation (see Table I). We also show the multiplicity distribution for $\alpha = 1$, which gives the best agreement with the parameterized model and Valentine's evaluation.

reaction. Thus, for this value, our results for the average γ multiplicity and average γ energy are in reasonable agreement with the latest measurements by Billnert *et al.* [13], as seen in Tables II and III.

Our results are summarized in Figs. 16, 17, and 18, where we compare our simulation with available experimental data and the parameterized model that describes the DANCE measurements very well. For the energy spectrum of the emitted γ rays, we do not reproduce the same overall quality of the agreement with the spectra of Billnert *et al.* [13] and Verbinski *et al.* [12] as for the thermal neutron induced reactions studied in this paper. At low energy, however, we reproduce better than for ^{235}U$(n_{\rm th}, f)$ and ^{239}Pu$(n_{\rm th}, f)$ the position of the peaks, albeit not always. Around 1.2 MeV, however, our calculation shows a broad peak that cannot be identified in the experimental data or is suppressed in similar calculations [47] that use a different procedure to match the level densities to the available experimental levels. The same broad peak appears in all our simulations presented in this paper, and it could be identified also, within error bars, in the experimental data for ^{235}U$(n_{\rm th}, f)$, shown in Fig. 8. In our simulations a large contribution for this peak comes from a handful of discrete transitions in ^{135}I, ^{137}Xe, and ^{139}Cs. We reproduce well the ENDF evaluated fission fragment yield for ^{135}I, but underproduce to some extent ^{137}Xe and ^{139}Cs. The simulations present the same peaks for different values of α, thus suggesting that the initial angular momentum does not play a significant role in this case, which can be understood, given that the spins of the states involved in the transitions are relatively low. Hence, it is possible that the information about longer-lived states (halflives of the order of nanoseconds) could be incomplete. Similar contributions in the same energy region could come from first to ground-state transitions in ^{134}Te, but because some higher-lying states have halflives of the order of the experimental time coincidence window, such transitions are suppressed. Finally, we note that the disagreement extends beyond 1.3 MeV, given that our calculation remains high with respect to the measurement up to about 4 MeV. Most of the contributions in this region come from statistical emissions thus making impossible to pinpoint a single culprit for the discrepancy.

In Fig 17, we plot the γ-ray multiplicity probability distribution, which is obtained in better agreement with the parameterized model and the Valentine evaluation than for ^{235}U$(n_{\rm th}, f)$ and ^{239}Pu$(n_{\rm th}, f)$ reactions. This is a consequence of the fact that the average γ multiplicities for our calculation and these models are in good agreement. The average multiplicity as a function of the initial fragment mass for ^{252}Cf(sf) is shown in Fig. 18(a), where we compare our results against data from Pleasonton *et al.* [11] and from a MPI report [48]. Thus, as in Fig. 10(a), we obtain a slowly increasing dependence on the initial fragment mass on the average γ multiplicity, while both data sets show a saw-tooth like behavior, more pronounced in the experiment by Pleasonton *et al.*

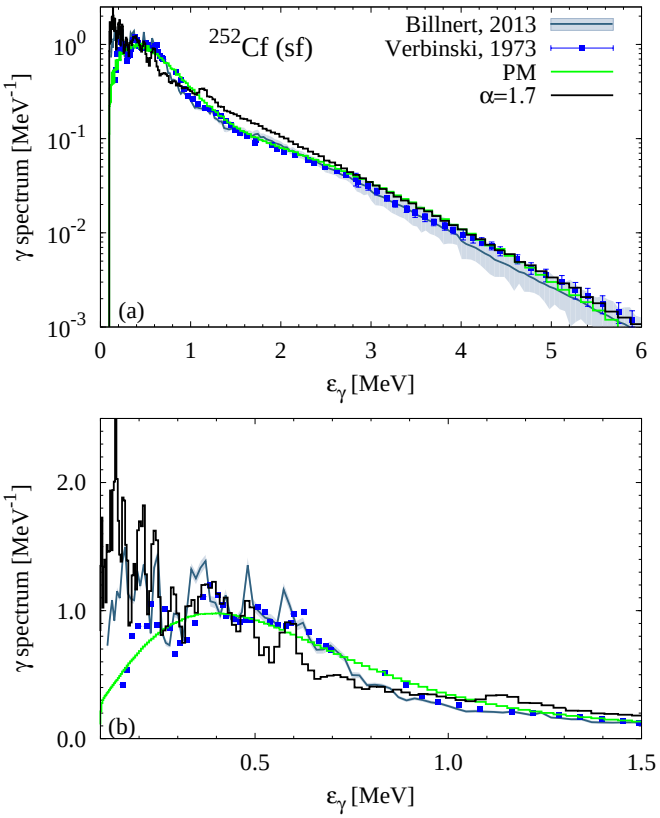

FIG. 16. (Color online) (a) The average prompt γ spectrum for the spontaneous fission of ^{252}Cf. Our calculation with $\alpha = 1.7$ is compared against the experimental spectra obtained by Verbinski [12] and Billnert [13], as well as against the parameterized model (PM) of Jandel et al. [15, 16]. (b) In the lower panel, we present, in linear scale, the low-energy part of the spectrum, where discrete transitions play a major role.

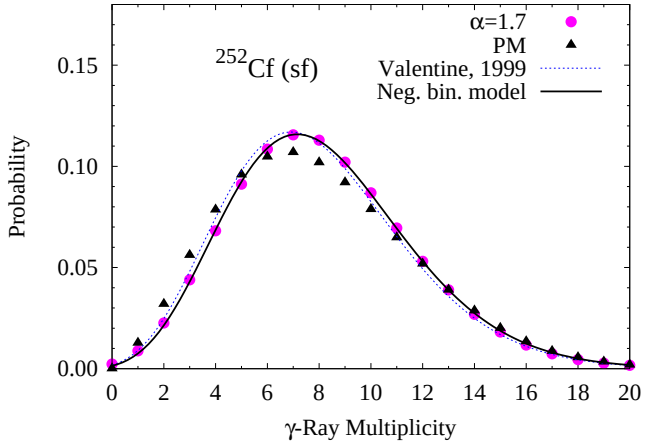

FIG. 17. (Color online) The prompt γ multiplicity distribution in MCHF for $\alpha = 1.7$ parameter compared against the parameterized model (PM), Valentine parametrization, and the negative binomial model with parameters fitted to our calculation (see Table I).

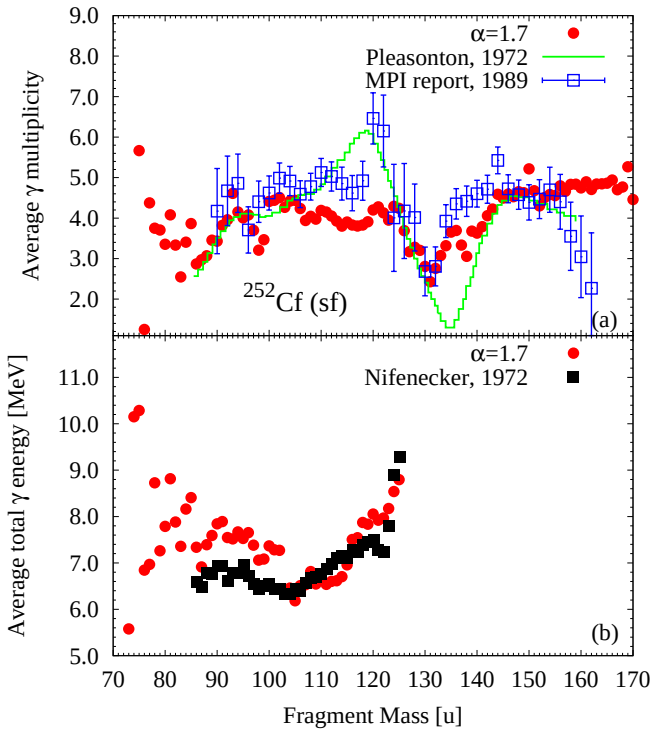

FIG. 18. (Color online) The average γ multiplicity (a) and average total γ energy per fission (b) as a function of fragment mass for ^{252}Cf (sf).

A somewhat better agreement can be observed for the average total γ energy per fission event as a function of the light fragment mass presented in Fig. 18(b). For more asymmetric configurations ($A_L < 100$), the calculations deviate from the experiment, but for masses above 100 we reproduce quite well the data of Nifenecker *et al.* [49].

V. SUMMARY AND OUTLOOK

We have presented our Monte Carlo Hauser-Feshbach simulations for selected quantities characterizing the prompt γ rays produced in several neutron-induced and spontaneous fission reactions: ^{235}U$(n_{\rm th}, f)$, ^{239}Pu$(n_{\rm th}, f)$ and ^{252}Cf(sf). We have presented results for the induced fission of ^{235}U with neutrons at 5.5 MeV incident energy, just below the second-chance fission threshold. The results for the energy spectra are in quantitatively good agreement with available experimental data. We were able to reproduce with fair accuracy the features in the spectrum arising from discrete transitions between low-lying states, although we observe a systematic shift from the experiment in the position of the peaks. Such low-energy structure of the spectra can be described only within the framework of the Hauser-Feshbach model that includes in the simulation experimental information about the branching ratios for transitions between low-energy states in fission fragments.

The Hauser-Feshbach model requires the use of a large number of adjustable parameters. Those are taken from systematics usually developed for long-lived nuclei. Thus, extrapolating the parameters to short-lived nuclei can translate into larger uncertainties. For other input, the experimental information is indirect. This is the case of the energy sharing mechanism, for which we adopt a simple model fitted to reproduce neutron observables. Similarly, no direct experimental information exists for the initial spin distribution of the primary fission fragments. Because the γ observables are very sensitive to the initial spin, we have adjusted our initial spin distributions to obtain the best agreement with the experiment for the average γ multiplicity, average γ energy and spectra. The neutrons are not completely insensitive to the spin, because a larger spin favors stronger neutron-γ competition. And even if their dependence on the spin parameter is weak, our calculations do not reproduce concomitantly both the neutron and the γ observables for the same initial spin distribution. For neutron observables, such as $\bar{\nu}$, it is preferable to increase the neutron-γ competition; this in turn can produce too many γ rays and worsen the description of γ observables. Such behavior suggests that using a global α parameter is an over-simplification, and a more realistic spin distribution is required.

Our approach is ideal for modeling correlations between the emitted particles, and can be used to extract exclusive quantities. In this paper, we have presented for the first time the multiplicity-dependent γ spectra, comparing our results with the parameterized model. The two simulations are in very good agreement. Furthermore, we can decompose the spectrum (and other observables) in precise contributions from individual fragments, which can help to estimate fission fragment yields. This approach is complementary to other theoretical [23, 24] and phenomenological [21] models developed for obtaining and improving the knowledge of the primary fission yields. Finally, the exclusive spectra can shed light on the quality of our calculations. In our current implementation, we reproduce qualitatively, but not quantitatively, trends observed in the exclusive experimental spectra stemming from specific initial fission fragments [50].

We currently work on extending our investigations to more fissile nuclei and higher neutron incident energy, up to 20 MeV. Data on primary fission fragment yields will be available from recent measurements with the SPIDER detector at LANSCE [51] and provide more reliable input to our calculation. Other improvements will include a more realistic initial spin distribution of the fission fragments, a more detailed model for the energy sharing between fragments.

ACKNOWLEDGMENTS

We thank S. Oberstedt, A. Oberstedt, and R. Billnert for providing their data on ^{252}Cf(sf) and ^{235}U$(n_{\rm th}, f)$,

and John Ullmann for useful discussions. We gratefully acknowledge the support of the U.S. Department of Energy through the LANL/LDRD Program. This work was performed at Los Alamos National Laboratory, under the auspices of the National Nuclear Security Administration of the U.S. Department of Energy at Los Alamos National Laboratory under contract No. DE-AC52-06NA25396. Work by MJ was supported by the U.S. Department of Energy, Office of Science, Nuclear Physics under the Early Career Award No. LANL20135009.

[1] J. C. Browne and F. S. Dietrich, Phys. Rev. C **10**, 2545 (1974).
[2] S. Lemaire, P. Talou, T. Kawano, M. B. Chadwick, and D. G. Madland, Phys. Rev. C **72**, 024601 (2005).
[3] Z. Na, D. Yi, Z. Chun-Lai, C. Jin-Xiang, and F. Tie-Shuan, Chinese Physics B **18**, 1413 (2009).
[4] P. Talou, B. Becker, T. Kawano, M. B. Chadwick, and Y. Danon, Phys. Rev. C **83**, 064612 (2011).
[5] A. Tudora, F.-J. Hambsch, and S. Oberstedt, Nucl. Phys. A **917**, 43 (2013).
[6] D. Blanchet, in *Mathematics and Computation 2005: International Topical Meeting on Mathematics and Computation, Supercomputing, Reactor Physics and Nuclear and Biological Applications* (2005).
[7] T. Kawano, P. Talou, M. B. Chadwick, and T. Watanabe, J. Nucl. Sci. Tech. **47**, 462 (2010).
[8] B. Becker, P. Talou, T. Kawano, Y. Danon, and I. Stetcu, Phys. Rev. C **87**, 014617 (2013).
[9] W. Hauser and H. Feshbach, Phys. Rev. **87**, 366 (1952).
[10] R. W. Peelle and F. C. Maienschein, Phys. Rev. C **3**, 373 (1971).
[11] F. Pleasonton, R. L. Ferguson, and H. W. Schmitt, Phys. Rev. C **6**, 1023 (1972); F. Pleasonton, Nucl. Phys. A **213**, 413 (1973).
[12] V. V. Verbinski, H. Weber, and R. E. Sund, Phys. Rev. C **7**, 1173 (1973).
[13] R. Billnert, F.-J. Hambsch, A. Oberstedt, and S. Oberstedt, Phys. Rev. C **87**, 024601 (2013).
[14] A. Oberstedt, T. Belgya, R. Billnert, R. Borcea, T. Bryś, W. Geerts, A. Göök, F.-J. Hambsch, Z. Kis, T. Martinez, S. Oberstedt, L. Szentmiklosi, K. Takàcs, and M. Vidali, Phys. Rev. C **87**, 051602 (2013).
[15] J. L. Ullmann, E. M. Bond, T. A. Bredeweg, A. Couture, R. C. Haight, M. Jandel, T. Kawano, H. Y. Lee, J. M. O'Donnell, A. C. Hayes, I. Stetcu, T. N. Taddeucci, P. Talou, D. J. Vieira, J. B. Wilhelmy, J. A. Becker, A. Chyzh, J. Gostic, R. Henderson, E. Kwan, and C. Y. Wu, Phys. Rev. C **87**, 044607 (2013).
[16] M. Jandel, T. A. Bredeweg, E. M. Bond, M. B. Chadwick, A. J. Couture, J. M. O'Donnell, M. M. Fowler, R. C. Haight, A. C. Hayes-Sterbenz, T. Kawano, R. S. Rundberg, G. Y. Rusev, P. Talou, I. Stetcu, J. L. Ullmann, D. J. Vieira, J. B. Wilhelmy, C.-Y. Wu, and J. A. Becker, *Prompt γ-ray emission in neutron induced fission of* ^{235}U, Tech. Rep. LA-UR-12-24975 (Los Alamos National Laboratory, 2013) to be published.
[17] S. Lemaire, P. Talou, T. Kawano, M. B. Chadwick, and D. G. Madland, Phys. Rev. C **73**, 014602 (2006).
[18] R. Vogt, J. Randrup, J. Pruet, and W. Younes, Phys. Rev. C **80**, 044611 (2009); R. Vogt, J. Randrup, D. A. Brown, M. A. Descalle, and W. E. Ormand, Phys. Rev. C **85**, 024608 (2012); R. Vogt and J. Randrup, Phys. Rev. C **87**, 044602 (2013).
[19] O. Litaize and O. Serot, Phys. Rev. C **82**, 054616 (2010).
[20] T. Wada, T. Asano, M. Hirokane, N. Carjan, and M. Rizea, Phys. Proc. **47**, 33 (2013), scientific Workshop on Nuclear Fission Dynamics and the Emission of Prompt Neutrons and Gamma Rays, Biarritz, France, 28-30 November 2012.
[21] K. H. Schmidt, S. Steinhäuser, C. Böckstiegel, A. Grewe, A. Heinz, A. R. Junghans, J. Benlliure, H. G. Clerc, M. de Jong, J. Müller, M. Pfützner, and B. Voss, Nucl. Phys. A **665**, 221 (2000).
[22] A. C. Wahl, *Systematics of fission-product yields*, report LA-13928 (Los Alamos National Laboratory, 2002).
[23] J. Randrup and P. Möller, Phys. Rev. Lett. **106**, 132503 (2011).
[24] W. Younes and D. Gogny, Phys. Rev. Lett. **107**, 132501 (2011); W. Younes, D. Gogny, and N. Schunck, in *Proceedings of the Fifth International Conference on ICFN5*, edited by J. H. Hamilton and A. V. Ramayya (World Scientific, 2013) p. 605.
[25] D. G. Madland and J. R. Nix, Nucl. Sci. Eng. **81**, 213 (1982).
[26] A. Tudora, Ann. Nucl. Eng. **33**, 1030 (2006).
[27] C. Morariu, A. Tudora, F.-J. Hambsch, S. Oberstedt, and C. Manailescu, J. Phys. G **39**, 055103 (2012).
[28] T. Ericson, Adv. Phys. **9**, 425 (1960).
[29] T. Ohsawa and T. Shibata, in *Nuclear Data for Science and Technology*, edited by S. M. Qaim (Springer-Verlag, 1991) p. 965.
[30] S. S. Kapoor and R. Ramanna, Phys. Rev. **133**, B598 (1964).
[31] H. Naik, S. P. Dange, and R. J. Singh, Phys. Rev. C **71**, 014304 (2005).
[32] J. B. Wilhelmy, E. Cheifetz, R. C. Jared, S. G. Thompson, H. R. Bowman, and J. O. Rasmussen, Phys. Rev. C **5**, 2041 (1972).
[33] M. M. Hoffman, Phys. Rev. **133**, B714 (1964).
[34] J. R. Huizenga and R. Vandenbosch, Phys. Rev. **120**, 1305 (1960); R. Vandenbosch and J. R. Huizenga, Phys. Rev. **120**, 1313 (1960).
[35] N. D. Dudey and T. T. Sugihara, Phys. Rev. **139**, B896 (1965).
[36] I. Stetcu, P. Talou, T. Kawano, and M. Jandel, Phys. Rev. C **88**, 044603 (2013).
[37] A. Koning and J. Delaroche, Nucl. Phys. A **713**, 231 (2003).
[38] D. Brink, Ph.D. thesis, Oxford (1955).
[39] J. Kopecky and M. Uhl, Phys. Rev. C **41**, 1941 (1990).
[40] R. Capote, M. Herman, P. Obložinský, P. Young, S. Goriely, T. Belgya, A. Ignatyuk, A. Koning, S. Hilaire, V. Plujko, M. Avrigeanu, O. Bersillon, M. Chadwick, T. Fukahori, Z. Ge, Y. Han, S. Kailas, J. Kopecky, V. Maslov, G. Reffo, M. Sin, E. Soukhovitskii, and P. Talou, Nucl. Data Sheets **110**, 3107 (2009), special Issue on Nuclear Reaction Data.
[41] A. Gilbert and A. G. W. Cameron, Can. J. Phys. **43**,

1446 (1965).
[42] T. Kawano, P. Talou, I. Stetcu, and M. Chadwick, Nucl. Phys. A **913**, 51 (2013).
[43] T. Valentine, *Evaluation of prompt fission gamma rays for use in simulating nuclear safeguard measurements*, Tech. Rep. ORNL/TM-1999/300 (1999).
[44] C. Romano, Y. Danon, R. Block, J. Thompson, E. Blain, and E. Bond, Phys. Rev. C **81**, 014607 (2010).
[45] H. Albinsson and L. Lindow, Tech. Rep. AE-398 (Aktiebolaget Atomenergi Studsvik, Nyköping, Sweden, 1970).
[46] F.-J. Hambsch, Private communication.
[47] D. Regnier, *Contribution à l'étude des gammas prompts de fission*, Ph.D. thesis, Université de Grenoble (2013).
[48] R. Schmid-Fabian, *Untersuchung der spontanen Spaltung von ^{252}Cf am Darmstadt-Heidelberger-Kristallkugel-Spectrometer*, Tech. Rep. MPI H 1989-V15 (Max-Planck-Intitut fuer Kernphysik Heidelberg, 1989).
[49] H. Nifenecker, C. Signarbieux, M. Ribrag, J. Poitou, and J. Matuszek, Nucl. Phys. A **189**, 285 (1972).
[50] A. Hotzel, P. Thirolf, C. Ender, D. Schwalm, M. Mutterer, P. Singer, M. Klemens, J. Theobald, M. Hesse, F. Gonnenwein, and H. Ploeg, Z. Phys. A. **356**, 299 (1996).
[51] F. Tovesson, C. W. Arnold, T. Bredeweg, M. Jandel, A. B. Laptev, K. Meierbachtol, A. Sierk, W. M., A. A. Hecht, D. Mader, B. R., U. Greife, B. Moore, D. Shields, and L. Snyder, in *Proceedings of the Fifth International Conference on ICFN5*, edited by J. H. Hamilton and A. V. Ramayya (World Scientific, 2013) p. 361.